JGR Atmospheres

Key Points:
- We assess the potential of CloudSat snowfall products for mapping snowfall rates at high spatial resolution across the Greenland Ice Sheet
- We find that our CloudSat climatologies capture seasonal and broad spatial patterns of snowfall rates accurately
- Compared with our CloudSat snowfall estimates, we find that regional and global climate models likely overestimate snowfall at the ice sheet margins

Supporting Information:
- Supporting Information S1

Correspondence to:
J. C. Ryan,
jonathan_ryan@brown.edu

Evaluation of CloudSat's Cloud-Profiling Radar for Mapping Snowfall Rates Across the Greenland Ice Sheet

Jonathan C. Ryan[1], Laurence C. Smith[1,2], Mengxi Wu[2], Sarah W. Cooley[1,2], Clément Miège[3], Lynn N. Montgomery[4], Lora S. Koenig[5], Xavier Fettweis[6], Brice P. Y. Noel[7], and Michiel R. van den Broeke[7]

[1]Institute at Brown for Environment and Society, Brown University, Providence, RI, USA, [2]Department of Earth, Environmental and Planetary Sciences, Brown University, Providence, RI, USA, [3]Department of Geography Rutgers, The State University of New Jersey, New Brunswick, NJ, USA, [4]Department of Atmospheric and Oceanic Science, University of Colorado Boulder, Boulder, CO, USA, [5]National Snow and Ice Data Center, University of Colorado Boulder, Boulder, CO, USA, [6]Laboratory of Climatology, Department of Geography, University of Liège, Liège, Belgium, [7]Institute for Marine and Atmospheric Research Utrecht, Utrecht University, Utrecht, the Netherlands

ABSTRACT The Greenland Ice Sheet is now the single largest cryospheric contributor to global sea-level rise yet uncertainty remains about its future contribution due to complex interactions between increasing snowfall and surface melt. Reducing uncertainty in future snowfall predictions requires sophisticated, physically based climate models evaluated with present-day observations. The accuracy of modeled snowfall rates, however, has yet to be systematically assessed because observations are sparse. Here, we produce high spatial resolution (15 km) snowfall climatologies (2006–2016) derived from CloudSat's 2C-SNOW-PROFILE product to evaluate climate model simulations of snowfall across the Greenland Ice Sheet. In comparison to accumulation datasets acquired from ice cores and airborne accumulation radar, we find that our CloudSat climatologies capture broad spatial patterns of snowfall in both the accumulation and ablation zones. By comparing our CloudSat snowfall climatologies with the Regional Atmospheric Climate Model Version 2.3p2 (RACMO2.3p2), Modèle Atmosphérique Régional 3.9 (MAR3.9), ERA5, and Community Earth System Model version 1 (CESM1), we demonstrate that climate models likely overestimate snowfall rates at the margins of the ice sheet, particularly in South, Southeast, and Northwest Greenland during autumn and winter. Despite this overestimation, there are few areas of the ice sheet where the models and CloudSat substantially disagree about the spatial pattern and seasonality of snowfall rates. We conclude that a combination of CloudSat snowfall observations and the latest generation of climate models has the potential to improve understanding of how snowfall rates respond to increasing air temperatures, thereby constraining one of the largest sources of uncertainty in Greenland's future contribution to global sea levels.

1. Introduction

The Greenland Ice Sheet has been losing mass at an accelerating rate since the start of the 21st century and is now the single largest cryospheric contributor to global sea-level rise (Chen et al., 2017; van den Broeke et al., 2016). The ice sheet's mass balance is primarily determined by the rate of accumulation (mainly due to snowfall) minus the rate of ablation (mainly due to surface meltwater runoff and solid ice discharge across grounding lines). Since the 1990s, observations and regional climate models (RCMs) agree that surface meltwater runoff and ice discharge have broadly increased in response to warmer ocean and summer air temperatures (Ahlstrøm et al., 2017; Mouginot et al., 2019; van den Broeke et al., 2016). Snowfall rates are also thought to positively correlate with air temperature, since warmer air carries exponentially more water vapor. However, discrepancies between observed and modeled accumulation (Koenig et al., 2016; Lewis et al., 2017; Overly et al., 2016) and between the models themselves (Ettema et al., 2009; Noël et al., 2018; Vernon et al., 2013) raise uncertainties about whether snowfall actually increased during this period of atmospheric warming. The response of snowfall to increasing air temperatures and the extent to which it can buffer the ice sheet in the next century therefore remains one of the largest uncertainties in future projections of Greenland Ice Sheet mass balance (van den Broeke et al., 2017).

Reducing uncertainties in modeled snowfall requires accurate empirical validation datasets that cover the entire ice sheet with fine temporal resolution. Since no such datasets exist, modeled snowfall rates are usually combined with modeled sublimation rates so that they can be evaluated against bulk accumulation rates measured by in situ ice/firn cores (Fettweis et al., 2017; Noël et al., 2018). Along with the inability to isolate the snowfall component of accumulation, comparisons between ice core and modeled accumulation have several additional limitations. First, the spatial extent of ice cores is limited to the accumulation zone where temperatures are below 0°C and annual snow layers are preserved. Yet observations from the dry, high-elevation interior of the ice sheet may not necessarily evaluate a model's ability to simulate accumulation at the wetter, ablating margins. Secondly, ice cores are almost always used to evaluate modeled accumulation at an annual to decadal temporal resolution (e.g., Fettweis et al., 2017; Noël et al., 2018), precluding evaluation of a model's ability to simulate accumulation over monthly or seasonal timescales (e.g., Castellani et al., 2015; Dibb & Fahnestock, 2004; Pettersen et al., 2018). Finally, most of the spatially distributed firn and ice cores were collected during the 1990s (Mosley-Thompson et al., 2001) and may not be representative of 21st century climate, a period of anomalously low surface mass balance. Therefore, comparisons between modeled and ice core accumulation rates may not accurately represent a climate model's ability to accurately simulate current and future ice sheet snowfall.

Contemporary snowfall observations with high temporal resolution are provided by automated weather stations (AWS; e.g., Fausto et al., 2018; Smeets et al., 2018). AWS are equipped with acoustic ranging sensors that record changes in surface elevation over hourly or shorter intervals (Steffen & Box, 2001). Positive changes in surface elevation can be converted to mass accumulation in water equivalent (w.e.) by multiplying by the snow density. However, snow density and its change over time are not typically measured by AWS so, in most cases, it is assumed or modeled. This step introduces substantial uncertainty in AWS-derived snowfall rates since snow compaction rates depend on numerous factors (e.g., air temperature, wind, and snowfall rates) and are difficult to model accurately (Herron & Langway, 1980). Isolating snowfall rates from changes in surface elevation is further complicated by melt, sublimation, and snow erosion, which can partially or fully remove the accumulated snow layer. Installing precipitation gauges, such as a bucket or upward-looking snow radar, on AWS would mitigate some of these problems, but these instruments are only installed on a few AWS at Summit Camp and near Kangerlussuaq, West Greenland (e.g., Castellani et al., 2015; Johansson et al., 2015). Snowfall measurements from all but a few AWS are therefore generally too inaccurate and isolated for validating snowfall rates from climate models across the ice sheet.

Observations with broader spatial coverage than ice cores and AWS can be acquired with near-surface scanning radars mounted on a sled or airborne platform. Isochronous reflecting horizons in radar echograms delineate annual or multiannual layers of snow accumulation that can be traced for hundreds of kilometers (e.g., Hawley et al., 2014; Koenig et al., 2016; Lewis et al., 2017; Medley et al., 2013; Miège et al., 2013; Overly et al., 2016). Ice-penetrating radar mounted on airborne platforms in particular has substantially improved the areal coverage of accumulation observations in the dry snow and percolation zones (van den Broeke et al., 2017). However, like most AWS, airborne accumulation radar estimates must assume or model the density of detected firn/snow layers to derive accumulation rates in w.e. (Koenig et al., 2016; Lewis et al., 2017; Overly et al., 2016). Correct interpretation of all radar measurements also requires further assumptions about melt intensity and age of the detected firn/snow layer. For example, near the ice sheet margins, internal layers from radar (usually collected in spring) do not represent 12 months of accumulation, since snow layers can either partially or completely melt during summer (Koenig et al., 2016). A more extensive accuracy assessment of accumulation rates derived from airborne accumulation radar is therefore required before these measurements can be treated as absolute "ground-truth," especially in the percolation and ablation zones.

Since 2006, National Aeronautics and Space Administration (NASA)'s CloudSat satellite has acquired snowfall observations with far better spatial coverage and temporal resolution than any of the in situ and field methods described so far (Stephens et al., 2008, 2018; Tanelli et al., 2008). Unlike the other techniques, which depend on accurate measurements of snow layer thickness and density, the cloud-profiling radar (CPR) onboard CloudSat can observe the w.e. mass of snow precipitating through the atmosphere before it has accumulated on the surface (Hiley et al., 2011; Kay et al., 2018; Kulie & Bennartz, 2009; Liu, 2008).

CloudSat therefore has potential to evaluate modeled snowfall in certain areas of the ice sheet (e.g., the margins), during certain time periods (e.g., the summer) for which few in situ observations exist.

Several studies have used CloudSat for model evaluation by producing gridded snowfall climatologies (i.e., mean annual snowfall rates) across the Arctic and Antarctica (Behrangi et al., 2016; Bennartz et al., 2019; Milani et al., 2018; Palerme et al., 2014; Palerme, Claud,et al., 2017; Palerme, et al., 2017). These climatologies have coarse spatial scales (e.g., 1 to 2° pixel size) to facilitate direct comparison with global climate models (GCMs). However, gridding CloudSat observations at this broad scale precludes meaningful comparison with in situ point measurements (e.g., Behrangi et al., 2016; Milani et al., 2018; Palerme et al., 2014, Palerme, Claud, et al., 2017, Palerme, Genthon, et al., 2017; Souverijns et al., 2018), making validation of coarsely gridded CloudSat snowfall climatologies difficult. The uncertainty associated with snowfall climatologies produced using CloudSat's CPR has therefore yet to be evaluated.

Here we produce finely gridded snowfall climatologies from CloudSat's 2C-SNOW-PROFILE product and assess their utility for evaluating modeled snowfall patterns and timing across the Greenland Ice Sheet. First, we compare instantaneous snowfall rates observed by CloudSat with coincident in situ snowfall rates as measured by (1) a precipitation gauge at KAN-B AWS in West Greenland and (2) the precipitation occurrence sensor system (POSS) at Summit Camp. We then evaluate how sampling size and distance impact the accuracy of our produced snowfall climatologies by aggregating multiple CloudSat profiles. Next we describe the production of two new CloudSat snowfall products gridded at a much finer spatial resolution (15×15 km) than previously attempted. The first product is a decadal (2006–2016) snowfall climatology averaged over the full 11-year CloudSat record. The second product includes four seasonal snowfall climatologies (March-April-May [MAM], June-July-August [JJA], September-October-November [SON], and December-January-February [DJF]) averaged over the full 11-year CloudSat record. We quantify the uncertainties of our snowfall climatologies in comparison to (1) 29 ice cores and (2) airborne accumulation radar data collected by multiple NASA Operation IceBridge campaigns (Koenig et al., 2016; Lewis et al., 2017). Finally, we compare our CloudSat snowfall climatologies with outputs of two RCMs (Regional Atmospheric Climate Model Version 2.3p2 [RACMO2.3p2] and Modèle Atmosphérique Régional [MAR3.9]), one GCM (the Community Earth System Model version 1, including the Community Atmosphere Model, version 5 [CESM1(CAM5)]) and an atmospheric reanalysis (ERA5). Discrepancies between these independent datasets allow us to identify where (e.g., regionally and altitudinally) and when (e.g., seasonally) modeled snowfall is most robust versus uncertain across the Greenland Ice Sheet.
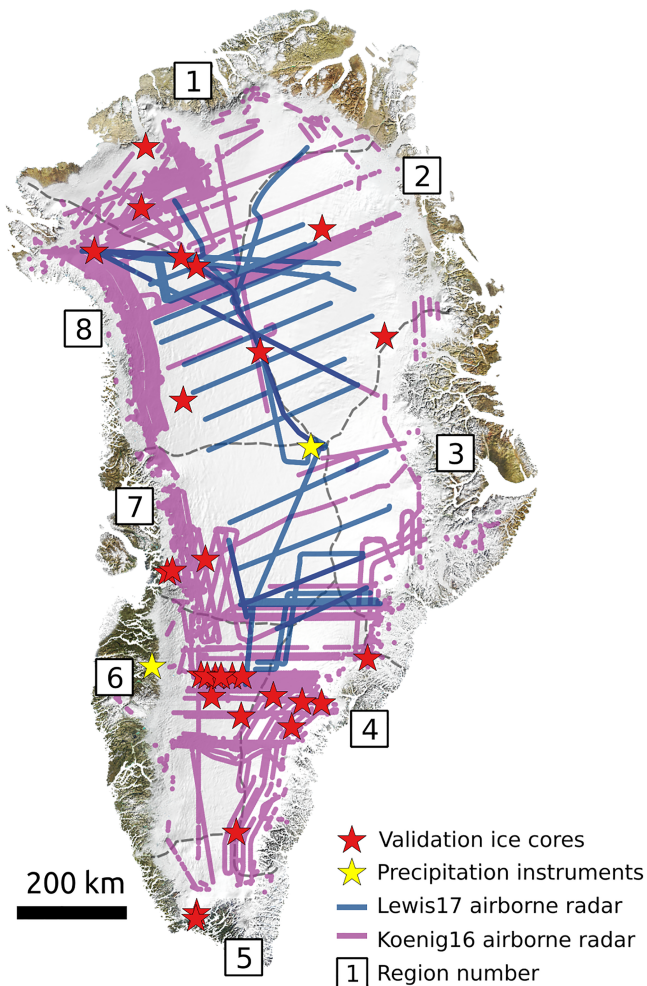
2. Data and Methods

2.1. CloudSat Satellite Data

2.1.1. Mission Summary

NASA's CloudSat mission was launched on 28 April 2006 to image the vertical structure of the Earth's clouds and precipitation (Stephens et al., 2002, 2008), joining the Afternoon Train (A-Train) satellite constellation between CALIPSO and Aqua. The A-Train sequence of satellites orbits the Earth Sun-synchronously at an altitude of 705 km with a repeat-pass of 16 days and a latitudinal range of 82.5°S to 82.5°N. In June 2006, CloudSat started collecting data, although a battery malfunction in 2011 necessitated a transition to a daylight-only operation mode and resulted in a multi-month (April to November) data gap. In June 2017, one of CloudSat's four reaction wheels displayed significant friction. Although the satellite could still conduct operations with three reaction wheels, the loss of a second wheel would have left CloudSat unable to maneuver or change its orientation. In February 2018, CloudSat safely exited its orbit to avoid possible collision with another A-Train satellite and is now in orbit below the A-Train.

2.1.2. 2C-SNOW-PROFILE Product

CloudSat is the first satellite to carry a 94-GHz (W-band) CPR, which measures backscatter from atmospheric targets (e.g., hydrometeors, ice crystals, and cloud droplets) at a vertical resolution of 240 m with a 1.8-km $\times$ 1.4-km horizontal footprint. Many studies have derived snowfall rates from CloudSat based on relationships between radar reflectivity (Z_e) and snowfall rate (S; Hiley et al., 2011; Hudak et al., 2008; Kulie & Bennartz, 2009; Liu, 2008; Matrosov & Heymsfield, 2008), and a standardized Level-2 product was released in February 2013 called 2C-SNOW-PROFILE (http://www.cloudsat.cira.colostate.edu/data-products/level-2c/2c-snow-profile Wood et al., 2014). This product incorporates a priori expectations of snow size distribution parameters and an optimal estimation method to derive snowfall rates in units

of snow w.e. (in units of mm/hr; Wood et al., 2014). The phase of precipitation is determined using vertical air temperature profiles from European Centre for Medium-Range Weather Forecasting (ECMWF) operational weather analysis in combination with a model of snow particle melting that allows up to ~15% melted mass fraction for snowfall. Surface snowfall rates over land are retrieved from the fifth bin above the surface (i.e., ~1,200 m) to remove contamination from ground clutter. Our study is based on Release 5, Version P1 of the 2C-SNOW-PROFILE product, which was released in June 2018. We used all 2C-SNOW-PROFILE data currently available (i.e., from June 2006 to October 2016) for analysis.

2.1.3. Data Preprocessing

The 2C-SNOW-PROFILE product has known uncertainties surrounding its assumptions about snow scattering properties, snow particle size distribution, and the Z_e-S relationship. Across Greenland, perhaps the greatest source of uncertainty is undetected ground clutter, which results in unrealistically high snowfall rates, particularly over steep topography (Behrangi et al., 2016; Palerme et al., 2019). To mitigate this effect, we removed most of spuriously high snowfall rate values using the retrieval status flag included with the 2C-SNOW-PROFILE product. However, we noticed that some spuriously high values were not flagged by the retrieval status flag. We therefore also removed all snowfall rates, which were greater than two standard deviations from a 50-km running median filter before gridding the 2C-SNOW-PROFILE product. This filter removed 3% of CloudSat observations and substantially reduced the impact of unrealistically high snowfall rates that were not flagged in the 2C-SNOW-PROFILE product (Figure S1 in the supporting information).

2.1.4. Accuracy Assessment of Individual Snowfall Events

We quantified the accuracy of the filtered 2C-SNOW-PROFILE product for individual snowfall events using in situ data from two ground-based instruments acquired simultaneously with 593 CloudSat overpasses. The first instrument is a precipitation gauge installed on the KAN-B AWS located near the margin of the ice sheet in West Greenland (Figure 1; Johansson et al., 2015; http://doi.pangaea.de/10.1594/PANGAEA.836178). The precipitation gauge contains antifreeze to melt captured solid precipitation and weighs the precipitation using a precision load cell with a vibrating wire transducer (Johansson et al., 2015). Precipitation data from this gauge are available from April 2011 onward. During this period, CloudSat overpassed within 50 km 102 times and detected 14 snowfall events. The second instrument is the POSS located at Summit Camp, the highest elevation on the ice sheet (Figure 1; Shupe et al., 2013; Castellani et al., 2015; Pettersen et al., 2018; https://arcticdata.io/catalog/view/doi:10.18739/A2TB83).

Figure 1. Locations of in situ and airborne observational datasets used to validate our CloudSat snowfall and accumulation rate products. Individual snowfall events were validated by the KAN-B automated weather station (AWS) precipitation gauge in West Greenland and the X-band Doppler radar precipitation occurrence sensor system located at Summit (yellow stars). Our decadal-averaged CloudSat accumulation climatology was validated using accumulation rates from 29 ice cores (red stars). We also compared our decadal-averaged CloudSat accumulation climatology to accumulation derived from airborne accumulation radar transects from Lewis et al. (2017; blue lines) and Koenig et al., (2016; purple lines). Numbers correspond to ice sheet regions defined by the Ice Sheet Mass Balance Intercomparison Exercise (IMBIE). 1: North; 2: Northeast; 3: East; 4: Southeast; 5: South; 6: Southwest; 7: West; 8: Northwest Greenland.

POSS is an X-band Doppler radar that measures w.e. snowfall rates by sampling the velocities and reflectivities of hydrometeors in approximately 1 m^3 of air directly above the transmitter and receiver (Pettersen et al., 2018). Due to the proximity of the sensor to the surface, POSS snowfall rates can be contaminated by blowing snow. To account for this, we excluded POSS snowfall rates with power unit values less than two, consistent with Pettersen et al. (2018). POSS data are available from September 2010 onward. During this period, CloudSat overpassed within 50 km 491 times and detected 110 snowfall events. To compare the datasets, we resampled the in situ snowfall rates to an hourly interval and selected the value that coincided closest to the timing of the CloudSat overpass. To ensure fair comparison with these in situ datasets, we only used CloudSat snowfall rates within 50 km of the KAN-B and Summit instrument installations.

2.1.5. Production of Snowfall Rate Climatologies

Decadal snowfall climatologies from the filtered 2C-SNOW-PROFILE product were derived by (1) averaging valid snowfall rates from individual CloudSat profiles within a specified search radius of a point-of-interest, (2) averaging these snowfall rates for each month, and (3) averaging all months to produce the 2006–2016 snowfall climatology. The intermediate step (2) is required because there are more snowfall data in summer than in winter after CloudSat switched to daylight-only operations mode in 2011. We compared the decadal-averaged snowfall rates derived from this method with accumulation rates observed at several validation sites where accumulation has been accurately measured by ice cores over the same period (Buchardt et al., 2012; Fausto et al., 2018; Iizuka et al., 2017; Macguth et al., 2016; Figure 1). We note that snowfall rates recorded by CloudSat are not necessarily equivalent to accumulation rates recorded by ice cores due to sublimation from the surface and from drifting snow particles. Therefore, we subtracted mean sublimation rates derived using an RCM (RACMO2.3p2; described in section 2.3) over the 2006–2016 study period from our CloudSat snowfall rates to ensure fair comparison between satellite and ice cores. When comparing with accumulation rates derived from ice cores and airborne accumulation radar in the next sections, we use these accumulation climatologies. When comparing with modeled snowfall simulated by regional and GCMs, we use the snowfall climatologies.

We also produced decadal and seasonal precipitation phase climatologies over the 2006–2016 study period using the 2C-PRECIP-COLUMN product (Figure S2). These climatologies were derived using the same sampling strategy as the snowfall climatologies but were produced by dividing the number of events classified as rain by the total number of precipitation events. We used these climatologies to identify potential sources of difference between observed and modeled snowfall.

2.1.6. Optimal Sample Size and Aggregation Area for CloudSat Snowfall Rate Retrievals

Comparing CloudSat accumulation climatologies to ice core estimates depends critically on the choice of search radius within which the satellite observations are sampled (Souverijns et al., 2018; van Tricht et al., 2016). A search radius too narrow may introduce error by reducing the sample size of CloudSat overpasses used to calculate mean snowfall rates at a specific point. On the other hand, a search radius too large may introduce error if CloudSat snowfall rate observations distal from the validation site are not representative of the validation site. To quantify this effect, we performed a sensitivity test for both search radius and sample size. First, we calculated mean snowfall rates using incrementally more CloudSat overpasses ranging from 10 to 200. To do this, we randomly selected CloudSat overpasses located within 45 km of each validation ice core site (Figure 1). Second, we calculated mean snowfall rates by increasing the search radius incrementally from 10 to 100 km. To do this, we randomly sampled CloudSat overpasses within specified distances from each validation ice core site while fixing the number of overpasses to 200. This analysis allowed us to assess how the sampling frequency and choice of search radius impacts the accuracy of snowfall rate climatologies produced by CloudSat.

We found, unsurprisingly, that the root-mean-square error (RMSE) uncertainty between CloudSat and ice core accumulation rates decreased with greater sample size and increased with larger search radius (Figure 2). On average, RMSE falls sharply from 84 to 9% as sample size increases from 10 to 100 (Figure 2a). Adding more than 100 samples reduces the uncertainty more gradually. Likewise, an RMSE of just 5% is introduced if only CloudSat observations within 50 km of the point-of-interest are included, rising to 24% if observations within 100 km are included (Figure 2b). This analysis demonstrates that sampling frequency and distance must be considered when aggregating multiple CloudSat profiles to produce climatologies.

In this study, we used a search radius of 45 km from the center of each grid cell when producing snowfall climatologies. This distance was chosen as an optimal trade-off between the uncertainty introduced by insufficient sampling of snowfall rates and the uncertainty introduced by the spatial heterogeneity of snowfall rates (Figure 3). We first constructed a grid with spatial resolution of 15×15 km across the Greenland Ice Sheet. This spacing was chosen so that we could make meaningful comparisons with both in situ point measurements and RCM outputs (RACMO2.3p2 and MAR3.9 have a grid resolution of 11 and 15 km, respectively). For each grid cell, we (1) averaged valid CloudSat snowfall rate observations from individual profiles within 45 km of the grid cell center, (2) averaged these snowfall rates for each month, and (3) averaged all months to produce a snowfall climatology for the 2006–2016 study period. We also produced four
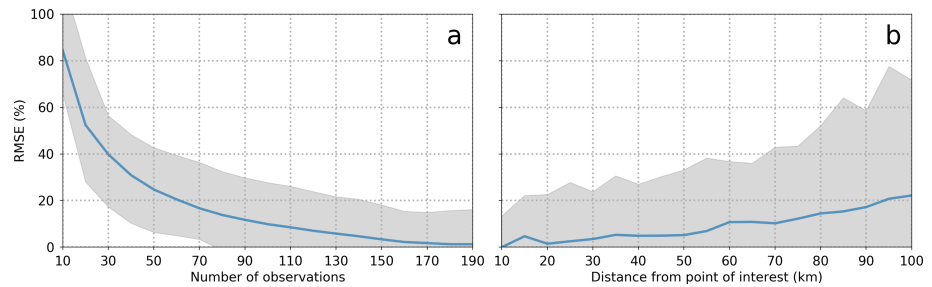
Figure 2. Root-mean-square error (RMSE) of CloudSat-derived mean annual accumulation rates (a) decreases as the number of satellite observations increases and (b) increases as the distance between satellite observations and a point of-interest increases. The plots demonstrate that sampling frequency and spatial averaging area must be considered when producing satellite-based snowfall/accumulation climatologies. Since sampling frequency decreases as the sampling search radius decreases, an optimal strategy for producing climatologies should consider using the smallest spatial averaging area that maintains at least 150 observations.

decadal snowfall climatologies (also 2006–2016) separating seasonal snowfall rates (e.g., spring [MAM], summer [JJA], autumn [SON], and winter [DJF]). Due to the reduced number of overpasses, these climatologies have slightly higher sampling uncertainty (mean RMSE in winter = 10.8%, mean RMSE in summer = 8.5%) than the decadal (2006–2016) snowfall climatology (mean RMSE = 4.2%).

2.2. Comparison With NASA Operation IceBridge Airborne Accumulation Radar

Once the sampling uncertainties were assessed, we next compared our CloudSat 2006–2016 snowfall climatology with two independent accumulation datasets collected by airborne radar during NASA's Operation IceBridge campaigns between 2009 and 2014 (Figure 1; Koenig et al., 2016; Lewis et al., 2017). The first dataset, hereafter termed "Lewis17," was collected using the University of Kansas Center for Remote Sensing of Ice Sheets (CReSIS) Accumulation Radar, which operated at a frequency of 600 to 900 MHz providing a vertical resolution of 50 cm in ice (Lewis et al., 2017; Rodriguez-Morales et al., 2014). Accumulation Radar signal can penetrate hundreds of meters in the dry-snow zone and tens of meters in the percolation zone, allowing deriving accumulation at decadal timescales (Lewis et al., 2017). The density between internal ice layers was calculated using a Herron and Langway (1980) depth-density model calibrated with two ice cores collected at Summit Station. We compared our decadal (2006–2016) CloudSat accumulation climatology with the shallowest accumulation layer detected by Lewis17, which represents the period 2004–2014. To account for the inexact temporal overlap between the two datasets, we compared snowfall rates averaged over the 2004–2014 period with the 2006–2016 period using RCM outputs. We found that the RMSE between the two periods was 0.03-m w.e. per year (a^{-1}; 8%) with a slight positive bias (+0.006 m w.e. a^{-1}). Therefore, although the two time periods do not overlap exactly, snowfall rates averaged over these two time periods are broadly comparable.

The second dataset, hereafter termed "Koenig16," was collected by the CReSIS ultrawideband Snow Radar (Koenig et al., 2016). Snow Radar has a higher frequency (2 to 8 GHz) than the Accumulation Radar and, while it is only able to penetrate tens of meters in the dry-snow zone and a few meters in the percolation and ablation zones, its centimeter-scale vertical resolution is capable of resolving annual snow layers (Koenig et al., 2016). The densities of the snow layers are assumed to be 338 kg/m^3 in the uppermost meter and are derived from modeled density profiles from MAR3.5.2 below 1 m. We compared our CloudSat 2006–2016 climatology with the accumulation layers corresponding to 2011 and 2012. To account for the inexact temporal overlap between the two datasets, we compared snowfall rates averaged over the 2011–2012 period with the 2006–2016 period using RCM outputs. We found that the RMSE
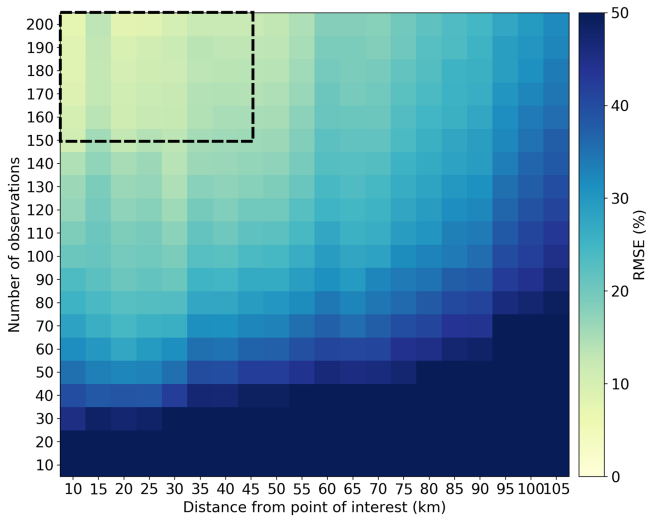
Figure 3. Pseudocolor plot showing how sampling frequency and sampling distance impact uncertainty in mean annual accumulation rates derived from CloudSat. Depending on the application, a tradeoff space between the two may be optimized to obtain the desired accuracy in accumulation rates. We find that a 45-km search radius enables high sample size (>150) across the entire Greenland Ice Sheet and maintains a sampling uncertainty of <5%.

between the two periods was 0.05 m w.e./a (11%) with a slight negative bias (-0.009 m w.e./a). We also note that Koenig16 represents ~10 months of accumulation because the lower boundary of the shallowest snow layer is assumed to represent peak melting conditions (i.e., 1 July $\pm$ 1 month) and the radar data were collected in Spring (April-May). In contrast, our CloudSat snowfall climatology represents 12 months of accumulation. These additional uncertainties are considered before conclusions are made about comparisons between CloudSat and Koenig16.

### 2.3. Comparison With Modeled Snowfall

We compared our decadal and seasonal CloudSat snowfall climatologies with snowfall outputs from two RCMs (MAR3.9 and RACMO2.3p2 with a spatial resolution of 15 and 11 km, respectively), one atmospheric reanalysis (ERA5 with a spatial resolution of ~25 km) and one GCM (CESM1[CAM5] or "CESM1" hereafter with a spatial resolution of around 120 km). All four model outputs have been used to estimate past, present (e.g., Fettweis et al., 2017; Noël et al., 2018), and future (e.g., Fettweis et al., 2013; Fyke et al., 2014; Vizcaíno et al., 2014) surface mass balance of the Greenland Ice Sheet. To compare these model outputs with our decadal and seasonal CloudSat snowfall products, we bilinearly resampled all products onto a common 15- $\times$ 15-km grid. We present the results of these comparisons above and below a 2,000 m `above sea level` (asl) threshold. This elevation threshold was chosen because almost all of the Lewis17 dataset is above 2,000 m asl, whereas the most of the Koenig16 dataset is below 2,000 m asl. We also divided the ice sheet into eight sectors as defined by the Ice sheet Mass Balance Intercomparison Exercise (IMBIE) to facilitate analysis of regional patterns (Figure 1). Dividing the comparisons in this way allowed us to identify where (e.g., regionally and altitudinally) and when (e.g., seasonally) modeled snowfall is most robust or uncertain across the Greenland Ice Sheet.

3. RESULTS

3.1. Accuracy Assessment

We find that CloudSat CPR-derived snowfall rates correlate well with snowfall rates measured by precipitation gauges at the margin (KAN-B) and summit (POSS) of the ice sheet (mean R^2 = 0.90; Figure 4a). In particular, CloudSat measured the intensity of two snowfall events (0.44 and 0.65 mm/hr) within $\pm$ 9% as compared to the precipitation gauge at KAN-B. These findings corroborate Lemonnier et al. (2019), who demonstrated that CloudSat measured snowfall rates of individual events with accuracies of -13 to $+22$% in comparison to microrain radar instruments located at the Dumont d'Urville and Princess Elisabeth stations in Antarctica. However, at Summit, we find that POSS observed 117 more snowfall events than CloudSat. The snowfall rates during these events tend to be small (mean = 0.0014 mm/hr) but cumulatively sum to 8% of the total snowfall at Summit. We hypothesize that CloudSat does not observe these snowfall events because they originate below 1,200 m above the surface (the height at which CloudSat observes snowfall) from shallow, mixed-phased clouds. Such snowfall regimes have been observed by CloudSat's CPR at Summit (McIlhattan et al., 2019; Pettersen et al., 2018). Therefore even though CloudSat appears to accurately observe the intensity of most snowfall events, it may systematically underestimate mean snowfall rates in regions where shallow precipitation events contribute a significant proportion of the total snowfall.

Indeed, when compared with the ice core validation sites, we find that our CloudSat 2006–2016 accumulation rate climatology generally underestimates accumulation (Figure 4b). This underestimation is particularly apparent in areas of the ice sheet which receive little snowfall. At high elevations, we attribute this underestimation to snowfall from shallow, mixed-phase clouds not observed by CloudSat. At lower elevations two other factors may be important. First, the backscatter measured by the CPR, which was designed to observe light snowfall, may saturate during heavy snowfall events due to its high frequency (94 GHz; Cao et al., 2014). Second, the phase of precipitation determined by the ECMWF vertical temperature profiles may lead to an overestimation of rainfall. During summer and below 2,000 m asl, we find that 23% of precipitation was classified as rainfall by the 2C-PRECIP-PROFILE product. In comparison, only 20% of precipitation was classified as rainfall by RACMO2.3p2 during the same period (Figure S2). Although this does not explain why CloudSat underestimates snowfall above 2,000 m asl, it could, at least partly, explain why CloudSat underestimates snowfall below 2,000 m asl. We note, however, that rain fraction varies substantially between models (Figure S2). MAR3.9, ERA5, and CESM1 classified 32%, 22%, and 25% of precipitation as rainfall during summer below 2,000 m asl. The phase of
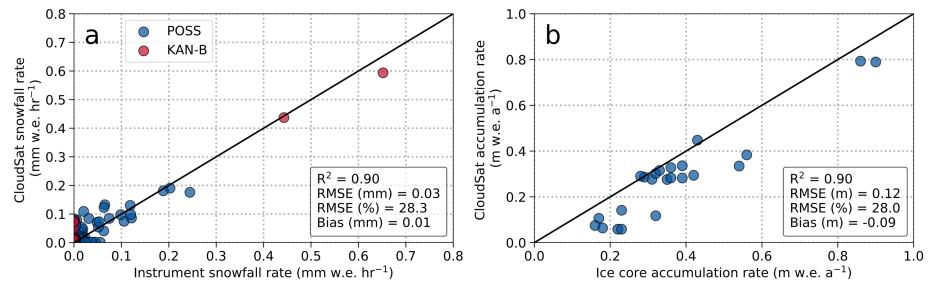
Figure 4. Comparisons between (a) individual snowfall events as detected by CloudSat (mm w.e./hr) and the KAN-B automated weather station precipitation gauge (red) and upward-looking Doppler radar precipitation occurrence sensor system (POSS) at Summit (blue) and (b) mean decadal accumulation rates as estimated from CloudSat and ice cores (m w.e./a; see Figure 1 for locations). Note that we used sublimation modeled by RACMO2.3p2 to convert CloudSat snowfall rates to accumulation rates.

precipitation therefore remains a large source of uncertainty in our comparisons of observed and modeled snowfall (e.g., Skofronick-Jackson et al., 2019).

After accounting for these biases, much of the remaining RMSE between our CloudSat 2006–2016 accumulation rate climatology and ice core validation sites can be explained by sampling uncertainties introduced when producing snowfall climatologies (Figure 5). These uncertainties are characterized by the strong latitudinal gradients in sampling frequency due to orbit convergence toward the poles. Considering all CloudSat observations over the entire 2006–2016 study period, grid cells in southern Greenland average 340 observations, whereas grid cells in northern Greenland average 2,541. Our sampling frequency analysis demonstrates that 340 observations are sufficient for producing an accurate mean snowfall rate over the 2006–2016 study period (Figure 2a), with a maximum uncertainty of ~5% due to sampling frequency and distance (Figure 5). Seasonal snowfall climatologies have higher uncertainty than the decadal climatology since each
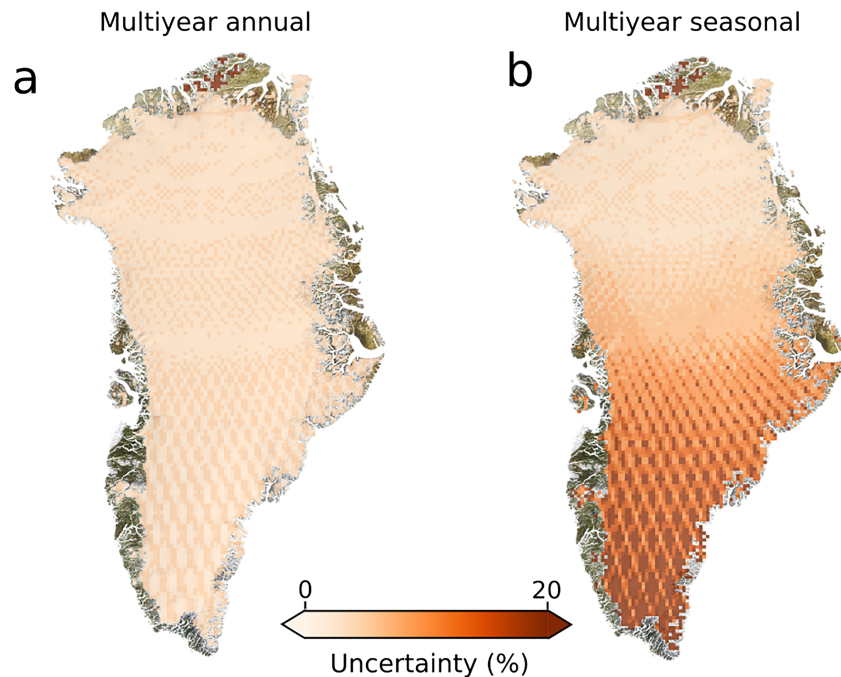
Figure 5. Spatial variability of CloudSat accumulation rate uncertainty due to sampling frequency. (a) The uncertainty due to sampling frequency in the decadal-averaged product is never higher than 5% because all grid cells receive at least 340 observations. (b) The uncertainty for the seasonally averaged product rises to up to 20% in South Greenland because some grid cells only receive 85 observations.
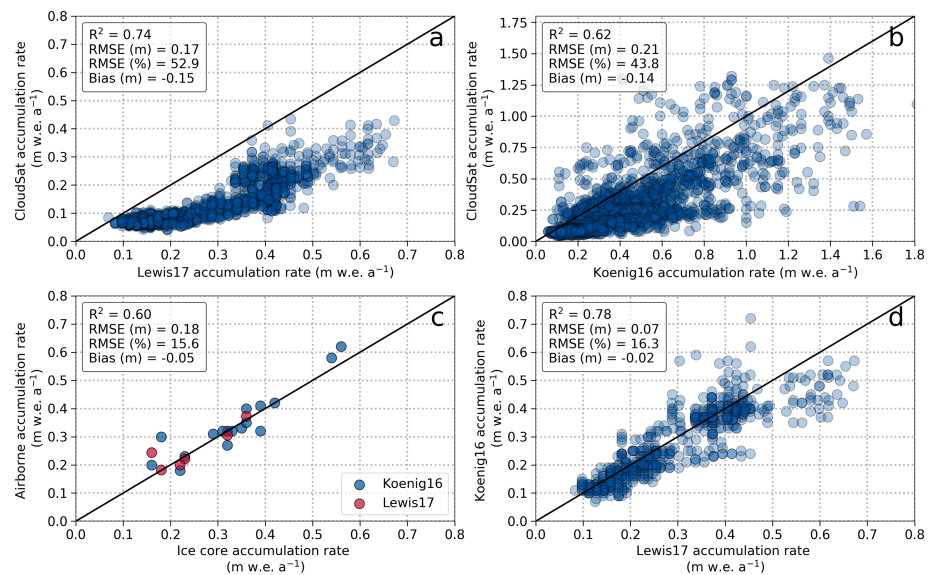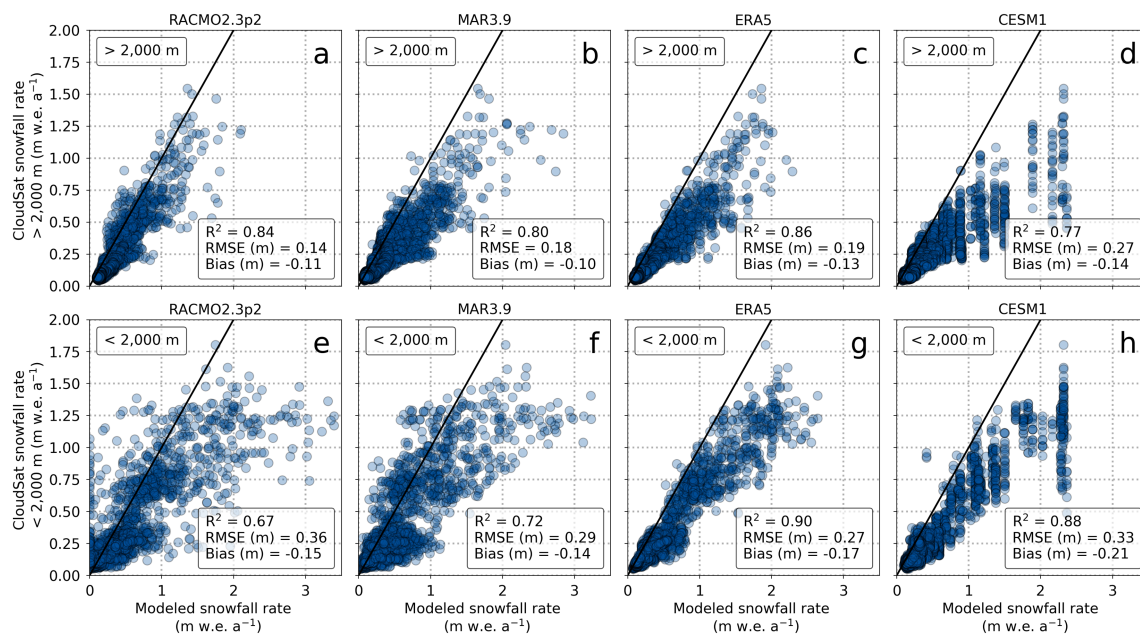
Figure 6. Comparison between (a) CloudSat and Lewis17 accumulation rates, (b) CloudSat and Koenig16 accumulation rates, (c) accumulation rates derived from both Lewis17 and Koenig16 with those derived from the validation ice cores, and (d) Lewis17 and Koenig16 accumulation rates. Each point represents a decadal-averaged accumulation rate in m w.e./a. Compared to airborne accumulation radar, we find that CloudSat systematically underestimates accumulation rates. The close agreement between the airborne accumulation radar and ice cores indicates that accumulation rates derived from accumulation radar contain no systematic biases.

aggregates only one quarter of the total number of CloudSat observations (Figure 5). Parsed into seasons, grid cells in North Greenland still receive 635 observations, whereas on average, grid cells in South Greenland only receive 85. The reduced number of observations introduces an uncertainty of up to 20% in the South Greenland seasonal snowfall climatology.

3.2. Comparison With Airborne Accumulation Radar at Decadal Timescale

Our decadal (2006–2016) CloudSat accumulation climatology compares well (R^2 of 0.74) with the decadal airborne accumulation radar datasets of Lewis et al. (2017) collected mostly above 2,000 m asl (Figure 6a), and with annual Koenig et al. (2016; $R^2 = 0.62$) collected mostly below 2,000 m asl (Figure 6b). The slightly worse correlation between CloudSat and Koenig16 is due to three main reasons. First, comparison between a single-year product (i.e., Koenig16) and a multiyear product (i.e., our CloudSat 2006-2016 climatology) introduces uncertainty due to interannual snowfall variability. Based on RCM outputs, we estimate that this could introduce uncertainties of up to ±11%. Second, Koenig16 assume that the density of the upper meter of snow is 338 kg/m^3, yet snow densities are known to vary across the ice sheet with a standard deviation of 44 kg/m^3 (Fausto et al., 2018). Third, many of the accumulation rates derived by Koenig16 are located at the margins of the ice sheet. Since melt occurs in these regions, the annual snow layers measured by Koenig16 might not represent a full 12 months of accumulation. For these reasons, discrepancies between CloudSat and Koenig16 likely do not reflect the actual accuracy of our CloudSat snowfall climatologies. Overall, even though there are fundamental differences between accumulation rates from airborne accumulation radar, which measures subsurface snow layering, and CloudSat radar, which measures atmospheric hydrometeor scattering, the strong correlations between the two approaches indicates that our CloudSat 2006–2016 climatology accurately captures spatial patterns of ice sheet accumulation (Figures 6a and 6b).

Despite these strong correlations, both radar-derived datasets confirm that CloudSat consistently underestimates accumulation rates across the ice sheet. Similar to the validation ice cores (Figure 4b), both the Lewis17 and Koenig16 datasets indicate that CloudSat underestimates accumulation by 0.15 and 0.14 m w.e./a, respectively (Figures 5a and 5b). This underestimation appears to be real since accumulation rates derived from airborne accumulation radar compare closely with accumulation rates derived from ice

Figure 7. Comparison between CloudSat and modeled snowfall rates (a–d) above and (e–h) below 2,000 m asl. Each point represents a snowfall rate (m w.e./a) averaged over the full 11-year (2006–2016) CloudSat record. (a and e) RACMO2.3p2 regional climate model, (b and f) MAR3.9 regional climate model (c and g) ERA5 reanalysis, and (d and h) CESM1 global climate model. In comparison to CloudSat, RACMO2.3p2, MAR3.9, and Community Earth System Model version 1 [CESM1] substantially overestimate snowfall at the margins of the ice sheet.

cores (Figure 6c) and with each other (Figure 6d). Our decadal CloudSat accumulation climatology is therefore probably not useful for direct model evaluation because, although it captures much of the spatial variability of accumulation across the Greenland Ice Sheet, the magnitude of accumulation is biased low.

3.3. Comparison With Modeled Snowfall at Decadal Timescale

Our CloudSat 2006–2016 snowfall climatology generally correlates well with modeled snowfall (Figure 7). Above 2,000 m asl, all models (RACMO2.3p2. MAR3.9, ERA5, and CESM1) correlate strongly with CloudSat (R^2 between 0.77 and 0.86; Figures 7a–7d). RACMO2.3p2 compares best with CloudSat at high elevations ($R^2 = 0.84$ and RMSE = 0.14 m w.e./a; Figure 7a), but strong correlations and relatively small residuals are also found between CloudSat, ERA5 and MAR3.9 (Figures 7b and 7c). CESM1, the coarse spatial resolution GCM, has lowest correlation ($R^2 = 0.77$) and largest RMSE in comparison to CloudSat (RMSE = 0.27 m w.e./a; Figure 7d). Although ERA5 correlates better with CloudSat below 2,000 m asl than above 2,000 m asl (R^2 of 0.90, Figure 7g), correlations between the RCMs and CloudSat worsen slightly at lower ice sheet elevations (R^2 of 0.67 and 0.72 for RACMO2.3p2 and MAR3.9, respectively, Figures 7e and 7f).

When compared with Lewis17, we find that all models underestimate accumulation above 2,000 m asl with RACMO2.3p2 underestimating the least (−0.06 m w.e./a) and MAR3.9 underestimating the most (−0.09 m w.e./a; Figure 8). This finding corroborates Overly et al. (2016), who found that older versions of the same RCMs (RACMO2.3 and MAR3.2) underestimated accumulation by −0.07 and −0.04 m w.e./a, respectively, in comparison to accumulation measured by airborne radar in central Greenland. Our analysis therefore confirms that RCMs and GCMs likely underestimate snowfall rates in the dry, high-elevation interior of the ice sheet.

When compared with CloudSat, we find that models likely overestimate snowfall at lower elevations (<2,000 m asl). This overestimation is greatest in regions of the ice sheet with high snowfall rates (>1.5 m w.e./a). For instance, in Southeast Greenland, RACMO2.3p2, MAR3.9, and ERA5 simulate decadal-averaged snowfall rates of up to 4.7, 3.2, and 2.6 m w.e./a, respectively, whereas maximum snowfall rates measured by CloudSat are only 1.8 m w.e./a. CESM1 also appears to substantially overestimate snowfall in lower elevations as compared to CloudSat (Figure 7h). Many of the residuals between CloudSat and the
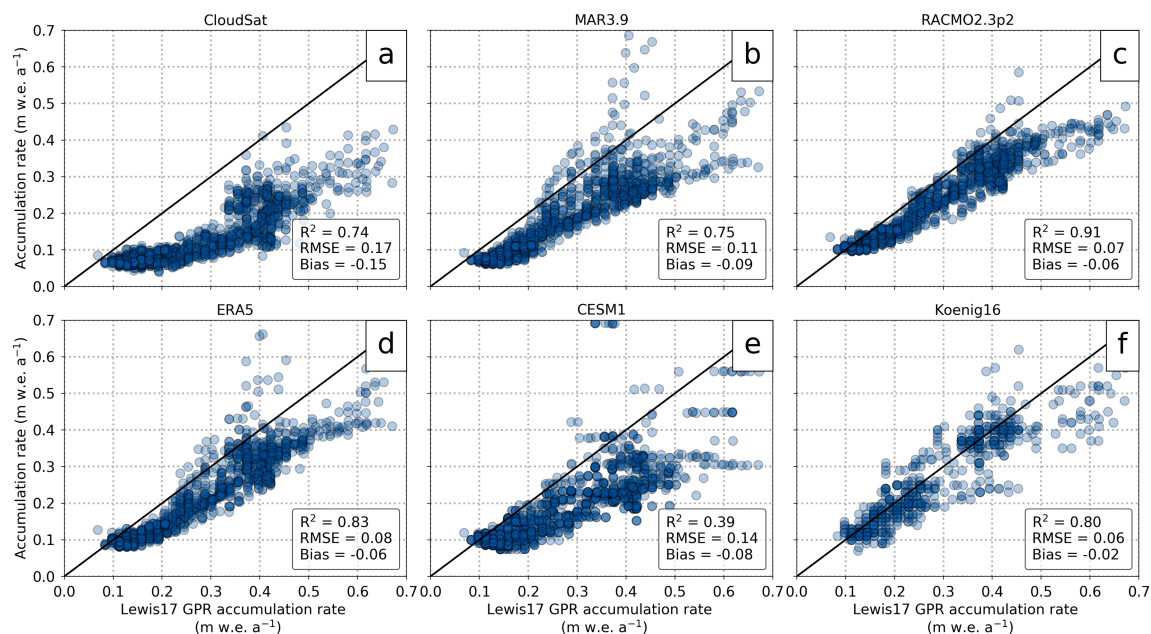
Figure 8. Comparisons between CloudSat and modeled accumulation rates with the airborne accumulation radar dataset of Lewis et al. (2017). Each point represents a decadal (2006–2016) average in m w.e./a. (a) CloudSat, (b) MAR3.9, (c) RACMO2.3p2, (d) ERA5, (e) CESM1, and (f) Koenig16. Note that nearly all the airborne accumulation radar data are from above 2,000 m asl. As compared to Lewis17, CloudSat and all the models systematically underestimate accumulation in the interior of the ice sheet.

climate models exceed the uncertainties of our CloudSat 2006–2016 snowfall climatology (Figures 4b and 6a), indicating that RCMs and GCMs likely overestimate snowfall rates in some low elevation regions near the ice sheet margins.

The spatial coverage of our CloudSat snowfall climatologies allows us to quantify this model overestimation in mass of w.e. After accounting for systematic bias in our CloudSat snowfall climatology (i.e., by adding 0.09 m w.e./a; Figures 4b and 6a), we find that RACMO2.3p2 and MAR3.9 overestimate snowfall below 2,000 m asl by 42.5 ± 47.4 Gt/a and 34.0 ± 47.4 Gt/a, respectively. This is equivalent to a $14.9 \pm 16.6\%$ and $12.2 \pm 16.9\%$ overestimation of snowfall below 2,000 m asl, and a $6.4 \pm 7.3\%$ and $5.2 \pm 7.4\%$ overestimation of the total ice sheet snowfall by RACMO2.3p2 and MAR3.9, respectively. RCM and GCM snowfall overestimation is predominantly located in the coastal regions of East and Southeast Greenland (IMBIE regions 3 and 4; Figures 9b, 9c, and 9e), although both RCMs also appear to overestimate snowfall in some coastal regions of West and Northwest Greenland (IMBIE regions 7 and 8; Figures 9b and 9c). Our bias-corrected CloudSat 2006–2016 snowfall climatology indicates that RACMO2.3p2 overestimates snowfall by 13.6 ± 5.6, 20.0 ± 8.6, and 8.4 ± 5.5 Gt/a at the margins of South, Southeast, and Northwest Greenland, respectively. Meanwhile MAR3.9 overestimates snowfall by 4.0 ± 5.6, 15.5 ± 9.2, and 7.9 ± 5.5 Gt/a in South, Southeast, and Northwest Greenland, respectively. These systematic biases raise uncertainty about modeled surface mass balance in these coastal regions of the Greenland Ice Sheet.

3.4. Comparison With Modeled Snowfall at Seasonal Timescale

Our CloudSat seasonal snowfall climatologies (MAM, JJA, SON, and DJF as averaged over the period 2006–2016) demonstrate that snowfall exhibits distinct variations at subannual timescales (Figure 10). Near the margins of the ice sheet, snowfall predominantly occurs during autumn and winter. Below 2,000 m asl, 29% and 30% of snow falls in autumn and winter, respectively, while only 24 and 18% falls in spring and summer, respectively (Figure 11). In the interior of the ice sheet, snowfall predominantly occurs during summer and autumn. Above 2,000 m asl, 26% and 31% of snow falls during the warmer summer and autumn, respectively, while 20% and 23% of snow falls during the colder spring and winter, respectively (Figure 12). At the margins of the ice sheet, the most pronounced snowfall seasonality is in Southeast Greenland where 42% of snow falls during winter and only 8% falls during summer. The most pronounced seasonality in the interior
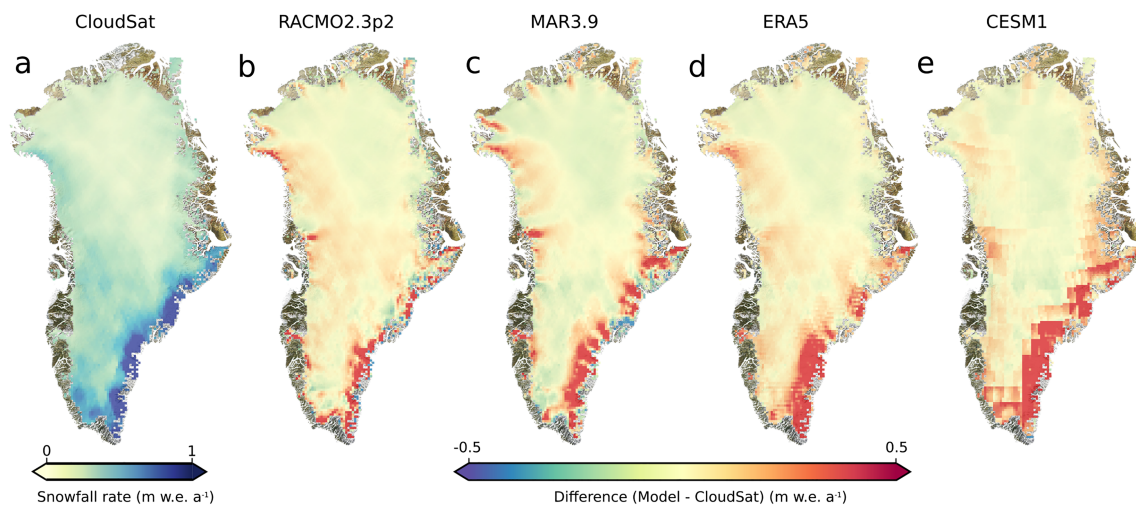
Figure 9. Spatial distribution of decadal averaged snowfall rates as (a) observed by CloudSat and compared with (b) RACMO2.3p2 regional climate model, (c) MAR3.9 regional climate model, (d) ERA5 reanalysis, (e) Community Earth System Model version 1 (CESM1) global climate model. The dashed lines delineate the eight IMBIE regions. Discrepancies between CloudSat and models are largest in Southeast Greenland and near the margins of the ice sheet. In East, Southeast, and South Greenland, all models overestimate snowfall in comparison to CloudSat.

of the ice sheet is in Northwest and North Greenland, where, on average, 39% of snow falls during the summer, which is more than double that which falls during winter (18%; Figure 12). Generally, Southwest, West, and Northeast Greenland exhibit less snowfall seasonality than North, Northwest, East, and Southeast Greenland.

RACMO2.3p2, MAR3.9, ERA5, and CESM1 all appear to capture the seasonality of snowfall observed by CloudSat relatively well (Figure 13). All models capture a satellite-observed reduction in snowfall between January and July near the ice sheet margins (Figure 13a) and increase in snowfall between March and September in the ice sheet interior (Figure 13b). However, they all appear to overestimate snowfall between September and December at the margins of the ice sheet.

4. DISCUSSION

Despite CloudSat′s narrow swath width (1.4 km) and relatively infrequent repeat overpass (16 days), this study demonstrates how CloudSat 2C-SNOW-PROFILE data may be used to produce fine-scale pan-Greenland snowfall climatologies that capture broad spatial patterns of snowfall (Figures 4b, 6a, and 9a). In contrast to previous studies, which assumed that coarse-scale grids were necessary to ensure sufficient sampling of CloudSat overpasses (Behrangi et al., 2016; Milani et al., 2018; Palerme et al., 2014, Palerme, Claud, et al., 2017, Palerme, Genthon, et al., 2017), our sampling frequency and distance analysis (section 2.1.6) suggests that accurate snowfall climatologies can be produced with relatively few (~150) CloudSat overpasses (Figure 2a). In this study, we therefore present CloudSat snowfall climatologies using relatively small sampling distances (<45 km) and grid resolutions (15- × 15-km pixel size). The fine resolution of these grids enables us to validate CloudSat snowfall climatologies for the first time using in situ observations and facilitates direct comparison with gridded RCMs.

We find that our decadal (2006–2016) CloudSat accumulation climatology has an uncertainty of $\pm$ 0.12 m w. e./a (equivalent to $\pm$ 28%; Figure 4b) relative to accumulation rates derived from ice cores. Much of this uncertainty is due to CloudSat′s systematic underestimation of accumulation (0.09 m w.e./a or 27%) likely due to missing near-surface snowfall events, and possibly because of instrument saturation during high magnitude snowfall events and overestimation of the rainfall fraction. After correcting for this systematic bias, the uncertainty of our decadal CloudSat climatology is reduced to $\pm$ 0.08 m w.e./a or $\pm$ 17%. The bias-corrected CloudSat climatology therefore provides an independent, remotely sensed source of snowfall and accumulation observations, useful as a stand-alone product or in combination with ice cores and airborne accumulation radar for systematic assessments of modeled snowfall. In particular, CloudSat
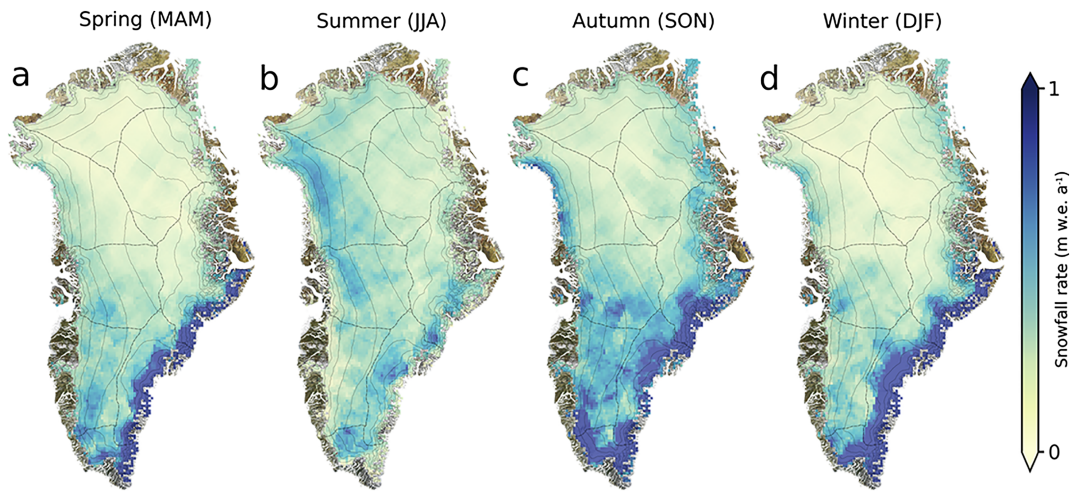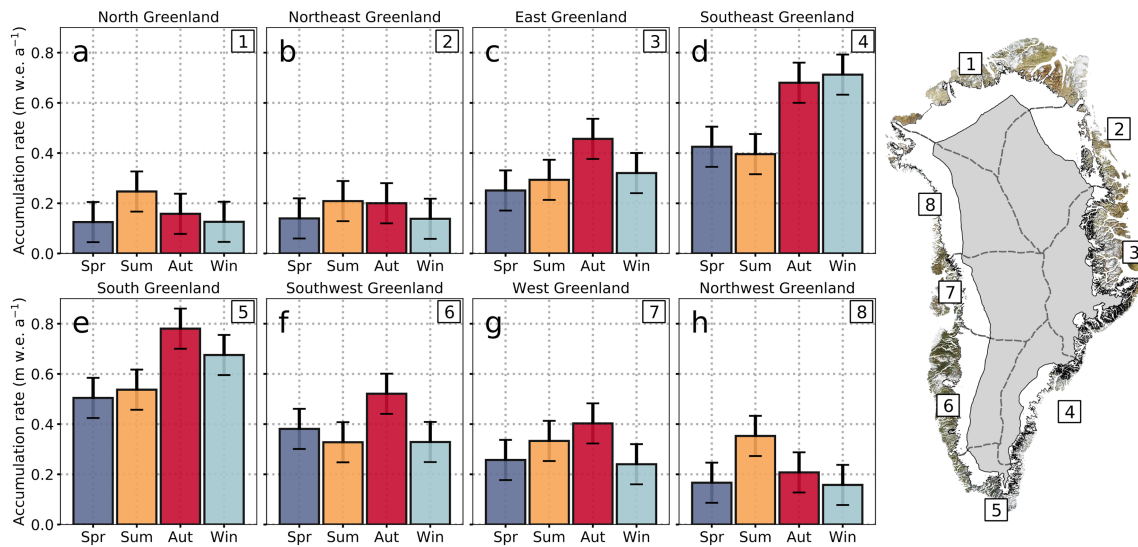
Figure 10. Seasonal distribution of CloudSat snowfall rates averaged over a decade (2006–2016). (a) Spring, (b) summer, (c) autumn, and (d) winter. The dashed lines delineate the eight Ice Sheet Mass Balance Intercomparison Exercise (IMBIE) regions.

observations may be used to quantify snowfall rates in regions (e.g., the margins of the ice sheet) and seasons (e.g., the summer) where few ice core or airborne accumulation radar observations exist.

Even after correcting for systematic bias in our CloudSat data product, we find that RCMs and GCMs likely overestimate snowfall rates below 2,000 m asl, especially near the ice margins of South, Southeast, and Northwest Greenland. This finding corroborates Koenig et al. (2016), who demonstrated that MAR3.8 overestimated accumulation in Southeast Greenland in comparison to Operation IceBridge snow radar observations. Yet while these airborne accumulation data document the direction of bias at specific point locations, our CloudSat snowfall climatology quantifies the full spatial extent of this bias. We find that RACMO2.3p2 and MAR3.9 likely overestimate snowfall below 2,000 m asl by 42.5 ± 47.4 Gt/a ($14.9 \pm 16.6\%$) and 34.0 ± 47.4 Gt/a ($12.2 \pm 16.9\%$), respectively. Furthermore, our seasonal CloudSat snowfall climatologies (Figures 11 and 12) demonstrate that most of this modeled snowfall overestimation occurs in autumn and winter. During these seasons, intense cyclonic activity induces heavy orographic precipitation in South,
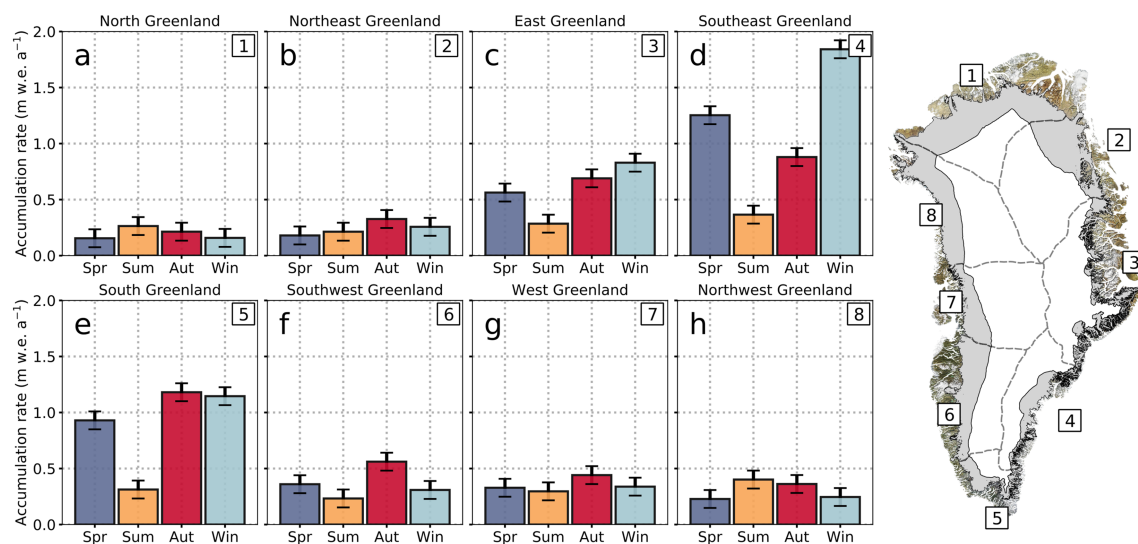
Figure 11. Seasonal distribution of snowfall in each of the eight Ice Sheet Mass Balance Intercomparison Exercise (IMBIE) regions below 2,000 m asl (grey shade in map). In East, Southeast, and South Greenland, almost all the snowfall occurs during autumn, winter, and spring since precipitation phase changes to rainfall in summer. In North, Northeast, West, and Northwest Greenland, snowfall exhibits less seasonal variability.

Figure 12. Seasonal distribution of snowfall in each of the eight Ice Sheet Mass Balance Intercomparison Exercise (IMBIE) regions above 2,000 m asl (grey shade in map). In colder, drier North, Northeast, and Northwest Greenland, most snowfall occurs during summer. In other regions of the ice sheet, most snowfall occurs in autumn or winter.

Southeast, and Northwest Greenland. Snowfall rates during these winter storms appear to be overestimated by RCMs and GCMs in comparison to CloudSat observations.

Model overestimation of snowfall near the ice sheet margins may have a compounding impact on modeled surface mass balance, because it may reduce the intensity of simulated ice sheet melt. If the thickness of the modeled winter snowpack is overestimated, bare ice will not be exposed until later in the season. Since snow has a much higher albedo than dark bare glacial ice, the ice sheet will absorb less shortwave radiation causing the models to underestimate surface melt in the ablation zone (Ryan et al., 2019). This compounding effect indicates that RACMO2.3p2 and MAR3.9 may actually overestimate net surface mass balance by more than that identified in this study.

Despite some systematic spatial and seasonal biases identified here, RACMO2.3p2 and MAR3.9 RCMs appear to accurately capture the spatial distribution and seasonal variation of Greenland Ice Sheet snowfall rates over the period 2006–2016 (Figures 9 and 13). Other than the Southeast Greenland margin, there are few areas of the ice sheet where the RCMs and CloudSat substantially disagree about snowfall rates (Figure 9). Notably, the RCMs perform accurately in the dry ice sheet interior, as evidenced by close
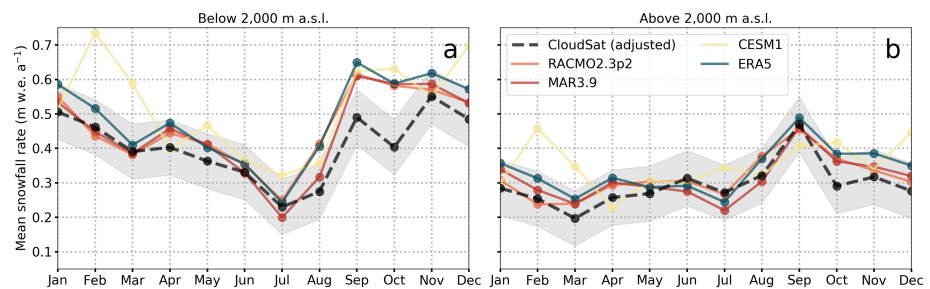
Figure 13. Comparison of CloudSat and modeled monthly snowfall rates averaged over a decade (2006–2016). (a) Monthly snowfall rates below 2,000 m asl. (b) Monthly snowfall rates above 2,000 m asl. The grey shade indicates uncertainty in CloudSat snowfall rates after bias correction (±0.08 m w.e./a or ± 17%). Generally, the seasonal variation in snowfall is captured by all models in comparison to our bias-corrected CloudSat snowfall climatology. However, below 2,000 m asl, the regional and global climate models appear to overestimate snowfall during autumn.

agreement between Lewis17 airborne accumulation radar data and RACMO2.3p2 above 2,000 m asl (R^2 of 0.91; Figure 8c). Both RACMO2.3p2 and MAR3.9 also appear to simulate the seasonal variability of snowfall accurately in comparison with CloudSat (Figure 13). This indicates that the RCMs capture the reduction in snowfall at the ice sheet margins due to phase change and the increase in snowfall in the ice sheet interior due to advection of warmer air inland. Therefore, with respect to snowfall biases at the margins of the ice sheet, RACMO2.3p2 and MAR3.9 should be able to simulate the future response of snowfall to future warmer air temperatures.

In addition to climate model evaluation, the CloudSat snowfall climatologies presented here may have many other potential applications. In the ablation zone, our CloudSat snowfall climatologies could be used in combination with satellite maps of bare ice extent and RCMs to understand how the thickness of the winter snowpack and melt combine to control the timing of snowline position and bare ice exposure, a key control on ice sheet surface runoff (Ryan et al., 2019). In the accumulation zone, our seasonal CloudSat climatologies could be useful for constraining the ratio of summer to winter snowfall, a metric that is particularly important for interpreting ice core isotope records (Cuffey & Steig, 1998). The individual CloudSat profiles may also be useful when combined with meteorological data from AWS for investigating dominant large-scale dynamic drivers of snowfall. For example, combining snowfall events from CloudSat with wind direction could be used to investigate the sources of moisture responsible for ice sheet snowfall. Likewise, combining air temperature with snowfall could be used to investigate how snowfall and snowlines respond to changing air temperatures. CloudSat may therefore provide important observations for understanding the response of Greenland Ice Sheet snowfall to climate change.

5. CONCLUSIONS

We investigated the potential of using 11 years (2006 to 2016) of CloudSat CPR data to produce accurate snowfall climatologies across the Greenland Ice Sheet. Our sampling size and frequency analysis demonstrated that snowfall climatologies can be produced at higher spatial resolution (15×15 km) than attempted by previous studies. The enhanced spatial resolution of the produced snowfall climatologies allowed direct comparison with "ground truth" datasets of ice sheet accumulation acquired from ice cores and airborne accumulation radar transects. Compared with these in situ measurements, we found that our CloudSat climatologies systematically underestimate snowfall, likely because CloudSat's CPR misses near-surface snowfall events, and possibly because of instrument saturation during heavy snowfall events, and overestimation of the rainfall fraction. Despite these biases, however, we found that our snowfall climatologies capture broad spatial patterns and seasonal fluctuations. Our CloudSat snowfall climatologies therefore provide an independent observational dataset for systematic evaluation of other observed or modeled snowfall products across the Greenland Ice Sheet. The data are available for scientific use at https://doi.pangaea.de/10.1594/PANGAEA.911416.

Our CloudSat snowfall climatologies are useful because they offer spatially extensive estimates of snowfall rates in areas of the ice sheet (e.g., the ablation zone) and during seasons (e.g., in summer) where few in situ snowfall records exist. In comparison to our satellite-based snowfall climatologies, we find that two RCMs (RACMO2.3p2 and MAR3.9), a meteorological reanalysis (ERA5), and a GCM (CESM1) likely overestimate snowfall rates at the margins of the ice sheet, particularly during autumn and winter in East, Southeast, and South Greenland. Other than these discrepancies, however, we find that RCMs accurately capture broad spatial and seasonal patterns of snowfall on the Greenland Ice Sheet. Going forward, a key use of our CloudSat snowfall observations could be to understand how snowfall rates respond to increasing air temperatures, thereby constraining one of the largest sources of uncertainty in Greenland's future contribution to global sea levels.

Author Contributions

JR conceptualized the project, developed the methodology, carried out the data analysis, and wrote the original manuscript. LS acquired the funding, provided supervision, and assisted with development of the methodology. MW, SW, CM, LM, LK, XF, BN, and MB assisted with development of the methodology, reviewed, and edited the manuscript.

Competing Interests

The authors declare that they have no competing interests.

Data and Materials Availability

The CloudSat 2C-SNOW-PROFILE product can be accessed online from the CloudSat data processing center maintained by Colorado State University: ftp://ftp1.cloudsat.cira.colostate.edu/2C-SNOW-PROFILE. P1_R05/. Our CloudSat snowfall climatologies are freely available for download at https://doi.pangaea.de/ 10.1594/PANGAEA.911416. Accumulation data derived from NASA's Operation IceBridge accumulation radar by Lewis et al. (2017) can be accessed from https://www.the-cryosphere.net/11/773/2017/tc-11-773- 2017-supplement.zip. Accumulation data derived from NASA's Operation IceBridge snow radar by Koenig et al. (2016) are available from https://doi.org/10.5067/FAZTWP500V70. The MARv3.9 outputs are available on ftp://climato.be/MARv3.9/Greenland/. RACMO2.3p2 outputs are available from the authors upon request and without conditions. CESM1 data can be accessed from http://www.cesm.ucar.edu/projects/ community-projects/LENS/. POSS data are available at NSF's Arctic Data Center: https://arcticdata.io/cat-alog/view/doi:10.18739/A2TB83. Data from the KAN-B weather station are available at http://doi.pan-gaea.de/10.1594/PANGAEA.836178.

References

Ahlstrøm, A. P., Petersen, D., Langen, P. L., Citterio, M., & Box, J. E. (2017). Abrupt shift in the observed runoff from the southwestern Greenland ice sheet. *Science Advances*, *3*(12), 1, e1701169–8. https://doi.org/10.1126/sciadv.1701169

Behrangi, A., Christensen, M., Richardson, M., Lebstock, M., Stephens, G., Huffman, G. J., et al. (2016). Status of high-latitude precipitation estimates from observations and reanalyses. *Journal of Geophysical Research-Atmospheres*, *121*(11), 6472–6488. https://doi.org/10.1002/ 2015JD023257

Bennartz, R., Fell, F., Pettersen, C., Shupe, M. D., & Schuettemeyer, D. (2019). Spatial and temporal variability of snowfall over Greenland from CloudSat observations. *Atmospheric Chemistry and Physics*, *19*, 8101–8121. https://doi.org/10.5194/acp-19-8101-2019

Box, J. E., Bromwich, D. H., Veenhuis, B. A., Bai, L. S., Stroeve, J. C., Rogers, J. C., et al. (2006). Greenland ice sheet surface mass balance variability (1988–2004) from calibrated polar MM5 output. *Journal of Climate*, *19*(12), 2783–2800. https://doi.org/10.1175/JCLI3738.1

Buchardt, S. L., Clausen, H. B., Vinther, B. M., & Dahl-Jensen, D. (2012). Investigating the past and recent δ18O-accumulation relationship seen in Greenland ice cores. *Climate of the Past*, *8*(6), 2053–2059. https://doi.org/10.5194/cp-8-2053-2012

Cao, Q., Hong, Y., Chen, S., Gourley, J. J., Zhang, J., & Kirstetter, P. E. (2014). Snowfall Detectability of NASA's CloudSat: the first cross-investigation of its 2C-Snow-Profile product and national multi-sensor mosaic QPE (NMQ) snowfall data. *Progress In Electromagnetics Research*, *148*, 55–61. https://doi.org/10.2528/pier14030405

Castellani, B. B., Shupe, M. D., Hudak, D. R., & Sheppard, B. E. (2015). The annual cycle of snowfall at Summit, Greenland. *Journal of Geophysical Research-Atmospheres*, *120*(13), 6654–6668. https://doi.org/10.1002/2015JD023072

Chen, X., Zhang, X., Church, J. A., Watson, C. S., King, M. A., Monselesan, D., et al. (2017). The increasing rate of global mean sea-level rise during 1993–2014. *Nature Climate Change*, *7*(7), 492–495. https://doi.org/10.1038/nclimate3325

Cuffey, K. M., & Steig, E. (1998). Isotopic diffusion in polar firn: implications for interpretation of seasonal climate parameters in ice-core records, with emphasis on central Greenland. *Journal of Glaciology*, *44*(1), 273–284. https://doi.org/10.3189/S0022143000002616

Dibb, J. E., & Fahnestock, M. (2004). Snow accumulation, surface height change, and firn densification at Summit, Greenland: Insights from 2 years of in situ observation. *Journal of Geophysical Research*, *109*, D24113. https://doi.org/10.1029/2003JD004300

Ettema, J., van den Broeke, M. R., van Meijgaard, E., van de Berg, W. J., Bamber, J. L., Box, J. E., & Bales, R. C. (2009). Higher surface mass balance of the Greenland ice sheet revealed by high-resolution climate modeling. *Geophysical Research Letters*, *36*, L12501. https://doi. org/10.1029/2009GL038110

Fausto, R. S., Box, J. E., Vandecrux, B., van As, D., Steffen, K., MacFerrin, M. J., et al. (2018). A snow density dataset for improving surface boundary conditions in Greenland Ice Sheet firn modeling. *Frontiers in Earth Science*, *6*, 1–10. https://doi.org/10.3389/feart.2018.00051

Fettweis, X., Franco, B., Tedesco, M., Van Angelen, J. H., Lenaerts, J. T. M., Van Den Broeke, M. R., & Gallée, H. (2013). Estimating the Greenland ice sheet surface mass balance contribution to future sea level rise using the regional atmospheric climate model MAR. *The Cryosphere*, *7*(2), 469–489. https://doi.org/10.5194/tc-7-469-2013

Fettweis, X., Box, J. E., Agosta, C., Amory, C., Kittel, C., Lang, C., et al. (2017). Reconstructions of the 1900–2015 Greenland ice sheet surface mass balance using the regional climate MAR model. *The Cryosphere*, *11*(2), 1015–1033. https://doi.org/10.5194/tc-11-1015-2017

Fyke, J. G., Vizcaíno, M., Lipscomb, W., & Price, S. (2014). Future climate warming increases Greenland ice sheet surface mass balance variability. *Geophysical Research Letters*, *41*(2), 470–475. https://doi.org/10.1002/2013GL058172

Hawley, R. L., Courville, Z. R., Kehrl, L. M., Lutz, E. R., Osterberg, E. C., Overly, T. B., & Wong, G. J. (2014). Recent accumulation variability in northwest Greenland from ground-penetrating radar and shallow cores along the Greenland Inland Traverse. *Journal of Glaciology*, *60*(220), 375–382. https://doi.org/10.3189/2014JoG13J141

Herron, M. M., & Langway, C. C. (1980). Firn densification: an empirical model. *Journal of Glaciology*, *25*(93), 87–89. https://doi.org/ 10.3189/S0022143000015239

Hiley, M. J., Kulie, M. S., & Bennartz, R. (2011). Uncertainty analysis for CloudSat snowfall retrievals. *Journal of Applied Meteorology and Climatology*, *50*(2), 399–418. https://doi.org/10.1175/2010JAMC2505.1

Hudak, D., Rodriguez, P., & Donaldson, N. (2008). Validation of the CloudSat precipitation occurrence algorithm using the Canadian C band radar network. *Journal of Geophysical Research*, *113*, D00A07. https://doi.org/10.1029/2008JD009992

Iizuka, Y., Miyamoto, A., Hori, A., Matoba, S., Furukawa, R., Saito, T., et al. (2017). A firn densification process in the high accumulation dome of southeastern Greenland. *Arctic, Antarctic, and Alpine Research*, *49*(1), 13–27. https://doi.org/10.1657/AAAR0016-034

Johansson, E., Berglund, S., Lindborg, T., Petrone, J., Van As, D., Gustafsson, L. G., et al. (2015). Hydrological and meteorological investigations in a periglacial lake catchment near Kangerlussuaq, west Greenland - Presentation of a new multi-parameter data set. *Earth System Science Data*, *7*(1), 93–108. https://doi.org/10.5194/essd-7-93-2015

Kay, J. E., L'Ecuyer, T., Pendergrass, A., Chepfer, H., Guzman, R., & Yettella, V. (2018). Scale-aware and definition-aware evaluation of modeled near-surface precipitation frequency using CloudSat observations. *Journal of Geophysical Research-Atmospheres*, *123*(8), 4294–4309. https://doi.org/10.1002/2017JD028213

Koenig, L. S., Ivanoff, A., Alexander, P. M., MacGregor, J. A., Fettweis, X., Panzer, B., et al. (2016). Annual Greenland accumulation rates (2009–2012) from airborne snow radar. *The Cryosphere*, *10*(4), 1739–1752. https://doi.org/10.5194/tc-10-1739-2016

Kulie, M. S., & Bennartz, R. (2009). Utilizing spaceborne radars to retrieve dry Snowfall. *Journal of Applied Meteorology and Climatology*, *48*(12), 2564–2580. https://doi.org/10.1175/2009JAMC2193.1

Lemonnier, F., Madeleine, J. B., Claud, C., Genthon, C., Durán-Alarcón, C., Palerme, C., et al. (2019). Evaluation of CloudSat snowfall rate profiles by a comparison with in situ micro-rain radar observations in East Antarctica. *The Cryosphere*, *13*(3), 943–954. https://doi.org/10.5194/tc-13-943-2019

Lewis, G., Osterberg, E., Hawley, R., Whitmore, B., Marshall, H. P., & Box, J. (2017). Regional Greenland accumulation variability from Operation IceBridge airborne accumulation radar. *The Cryosphere*, *11*(2), 773–788. https://doi.org/10.5194/tc-11-773-2017

Liu, G. (2008). Deriving snow cloud characteristics from CloudSat observations. *Journal of Geophysical Research*, *113*, D00A09. https://doi.org/10.1029/2007JD009766

Macguth, H., Thomsen, H. H., Weidick, A., Ahlstrøm, A. P., Abermann, J., Andersen, M. L., et al. (2016). Greenland surface mass-balance observations from the ice-sheet ablation area and local glaciers. *Journal of Glaciology*, *62*(235), 861–887. https://doi.org/10.1017/jog.2016.75

Matrosov, S. Y., & Heymsfield, A. J. (2008). Estimating ice content and extinction in precipitating cloud systems from CloudSat radar measurements. *Journal of Geophysical Research*, *113*, D00A05. https://doi.org/10.1029/2007JD009633

McIlhattan, E. A., Pettersen, C., Wood, N. B., & L'Ecuyer, T. S. (2019). Satellite observations of snowfall regimes over the Greenland Ice Sheet. *The Cryosphere Discussions*. https://doi.org/10.5194/tc-2019-223

Medley, B., Joughin, I., Das, S. B., Steig, E. J., Conway, H., Gogineni, S., et al. (2013). Airborne-radar and ice-core observations of annual snow accumulation over Thwaites Glacier, West Antarctica confirm the spatiotemporal variability of global and regional atmospheric models. *Geophysical Research Letters*, *40*(14), 3649–3654. https://doi.org/10.1002/grl.50706

Miège, C., Forster, R. R., Box, J. E., Burgess, E. W., Mcconnell, J. R., Pasteris, D. R., & Spikes, V. B. (2013). Southeast Greenland high accumulation rates derived from firn cores and ground-penetrating radar. *Annals of Glaciology*, *54*(63), 322–332. https://doi.org/10.3189/2013AoG63A358

Milani, L., Kulie, M. S., Casella, D., Dietrich, S., L'Ecuyer, T. S., Panegrossi, G., et al. (2018). CloudSat snowfall estimates over Antarctica and the Southern Ocean: An assessment of independent retrieval methodologies and multi-year snowfall analysis. *Atmospheric Research*, *213*, 121–135. https://doi.org/10.1016/j.atmosres.2018.05.015

Mosley-Thompson, E., McConnell, J. R., Bales, R. C., Li, Z., Lin, P., Steffen, K., et al. (2001). Local to regional-scale variability of annual net accumulation on the Greenland ice sheet from PARCA cores Regional Climate Assessment opportunity to assess local to regional variability of annual accumulation rates over the Greenland Ice Sheet. *Journal of Geophysical Research*, *106*(D24), 33,839–33,851. https://doi.org/10.1029/2001JD900067

Mouginot, J., Rignot, E., Bjørk, A. A., van den Broeke, M., Millan, R., Morlighem, M., et al. (2019). Forty-six years of Greenland Ice Sheet mass balance from 1972 to 2018. *Proceedings of the National Academy of Sciences*, *116*(19), 9239–9244. https://doi.org/10.1073/pnas.1904242116

Noël, B., van de Berg, W. J., van Wessem, J. M., van Meijgaard, E., & van As, D. (2018). Modelling the climate and surface mass balance of polar ice sheets using RACMO2—Part 1: Greenland (1958–2016). *The Cryosphere*, *2013*, 811–831. https://doi.org/10.5194/tc-12-811-2018

Overly, T. B., Hawley, R. L., Helm, V., Morris, E. M., & Chaudhary, R. N. (2016). Greenland annual accumulation along the EGIG line, 1959-2004, from ASIRAS airborne radar and neutron-probe density measurements. *The Cryosphere*, *10*(4), 1679–1694. https://doi.org/10.5194/tc-10-1679-2016

Palerme, C., Claud, C., Dufour, A., Genthon, C., Wood, N. B., & L'Ecuyer, T. (2017). Evaluation of Antarctic snowfall in global meteorological reanalyses. *Atmospheric Research*, *190*, 104–112. https://doi.org/10.1016/j.atmosres.2017.02.015

Palerme, C., Claud, C., Wood, N. B., L'Ecuyer, T., & Genthon, C. (2019). How does ground clutter affect CloudSat snowfall retrievals over ice sheets? *IEEE Geoscience and Remote Sensing Letters*, *16*(3), 342–346. https://doi.org/10.1109/LGRS.2018.2875007

Palerme, C., Genthon, C., Claud, C., Kay, J. E., Wood, N. B., & L'Ecuyer, T. (2017). Evaluation of current and projected Antarctic precipitation in CMIP5 models. *Climate Dynamics*, *48*(1–2), 225–239. https://doi.org/10.1007/s00382-016-3071-1

Palerme, C., Kay, J. E., Genthon, C., L'Ecuyer, T., Wood, N. B., & Claud, C. (2014). How much snow falls on the Antarctic ice sheet? *The Cryosphere*, *8*(4), 1577–1587. https://doi.org/10.5194/tc-8-1577-2014

Pettersen, C., Bennartz, R., Merrelli, A. J., Shupe, M. D., Turner, D. D., & Walden, V. P. (2018). Precipitation regimes over central Greenland inferred from 5 years of ICECAPS observations. *Atmospheric Chemistry and Physics*, *18*(7), 4715–4735. https://doi.org/10.5194/acp-18-4715-2018

Rodriguez-Morales, F., Gogineni, S., Leuschen, C. J., Paden, J. D., Li, J., Lewis, C. C., et al. (2014). Advanced multifrequency radar instrumentation for polar Research. *IEEE Transactions on Geoscience and Remote Sensing*, *52*(5), 2824–2842. https://doi.org/10.1109/TGRS.2013.2266415

Ryan, J. C., Smith, L. C., Van As, D., Cooley, S. W., Cooper, M. G., Pitcher, L. H., & Hubbard, A. (2019). Greenland Ice Sheet surface melt amplified by snowline migration and bare ice exposure. *Science Advances*, *5*(3), eaav3738. https://doi.org/10.1126/sciadv.aav3738

Shupe, M. D., Turner, D. D., Walden, V. P., Bennartz, R., Cadeddu, M. P., Castellani, B. B., et al. (2013). High and dry: New observations of tropospheric and cloud properties above the Greenland Ice Sheet. *Bulletin of the American Meteorological Society*, *94*, 169–186. https://doi.org/10.1175/BAMS-D-11-00249.1

Skofronick-Jackson, G., Kulie, M., Milani, L., Munchak, S. J., Wood, N. B., & Levizzani, V. (2019). Satellite estimation of falling snow: A global precipitation measurement (GPM) Core Observatory perspective. *Journal of Applied Meteorology and Climatology*, *58*, 1429–1448. https://doi.org/10.1175/JAMC-D-18-0124.1

Smeets, P. C. J. P., Kuipers Munneke, P., van As, D., van den Broeke, M. R., Boot, W., Oerlemans, H., et al. (2018). The K-transect in west Greenland: Automatic weather station data (1993–2016). *Arctic, Antarctic, and Alpine Research*, *50*(1), S100002. https://doi.org/10.1080/15230430.2017.1420954

Souverijns, N., Gossart, A., Lhermitte, S., Gorodetskaya, I. V., Grazioli, J., Berne, A., et al. (2018). Evaluation of the CloudSat surface snowfall product over Antarctica using ground-based precipitation radars. *The Cryosphere*, *12*(12), 3775–3789. https://doi.org/10.5194/tc-12-3775-2018

Steffen, K., & Box, J. (2001). Surface climatology of the Greenland ice sheet: Greenland Climate Network 1995-1999. *Journal of Geophysical Research*, *106*(12), 33,951–33,964. https://doi.org/0148-0227/01/2001JD900161$09.00

Stephens, G., Winker, D., Pelon, J., Trepte, C., Vane, D., Yuhas, C., et al. (2018). Cloudsat and Calipso within the A-Train: Ten years of actively observing the earth system. *Bulletin of the American Meteorological Society*, *99*(3), 569–581. https://doi.org/10.1175/BAMS-D-16-0324.1

Stephens, G. L., Vane, D. G., Boain, R. J., Mace, G. G., Sassen, K., Wang, Z. E., et al., & the CloudSat Science Team (2002). The CloudSat mission and the A-Train - A new dimension of space-based observations of clouds and precipitation. *Bulletin of the American Meteorological Society*, *83*(12), 1771–1790. https://doi.org/10.1175/Bams-83-12-1771

Stephens, G. L., Vane, D. G., Tanelli, S., Im, E., Durden, S., Rokey, M., et al. (2008). CloudSat mission: Performance and early science after the first year of operation. *Journal of Geophysical Research*, *113*, D00A18. https://doi.org/10.1029/2008JD009982

Tanelli, S., Durden, S. L., Im, E., Pak, K. S., Reinke, D. G., Partain, P., et al. (2008). CloudSat's cloud profiling radar after two years in orbit: Performance, calibration, and processing. *IEEE Transactions on Geoscience and Remote Sensing*, *46*(11), 3560–3573. https://doi.org/10.1109/TGRS.2008.2002030

van den Broeke, M. R., Box, J., Fettweis, X., Hanna, E., Noël, B., Tedesco, M., et al. (2017). Greenland Ice Sheet surface mass loss: Recent developments in observation and modeling. *Current Climate Change Reports*, *3*(4), 345–356. https://doi.org/10.1007/s40641-017-0084-8

van den Broeke, M. R., Enderlin, E. M., Howat, I. M., Kuipers Munneke, P., Noël, B. P. Y., Jan Van De Berg, W., et al. (2016). On the recent contribution of the Greenland ice sheet to sea level change. *The Cryosphere*, *10*(5), 1933–1946. https://doi.org/10.5194/tc-10-1933-2016

van Tricht, K., Lhermitte, S., Gorodetskaya, I. V., & Van Lipzig, N. P. M. (2016). Improving satellite-retrieved surface radiative fluxes in polar regions using a smart sampling approach. *The Cryosphere*, *10*(5), 2379–2397. https://doi.org/10.5194/tc-10-2379-2016

Vernon, C. L., Bamber, J. L., Box, J. E., van den Broeke, M. R., Fettweis, X., Hanna, E., & Huybrechts, P. (2013). Surface mass balance model intercomparison for the Greenland ice sheet. *The Cryosphere*, *7*(2), 599–614. https://doi.org/10.5194/tc-7-599-2013

Vizcaíno, M., Lipscomb, W. H., Sacks, W. J., & van den Broeke, M. (2014). Greenland surface mass balance as simulated by the Community Earth System Model. Part II: Twenty-First-Century Changes. *Journal of Climate*, *27*(1), 215–226. https://doi.org/10.1175/JCLI-D-12-00588.1

Wood, N. B., L'Ecuyer, T. S., Heymsfield, A. J., Stephen, G. L., Hudak, D. R., & Rodriguez, P. (2014). Estimating snow microphysical properties using collocated multisensor observations. *Journal of Geophysical Research-Atmospheres*, *119*(14), 8941–8961. https://doi.org/10.1002/2013JD021303